

Suha A. Mohammed

Mechanical Engineering
Department, University of
Technology
Baghdad, Iraq
shawsuha@yahoo.com

Ekhlas M. Fayyadh

Mechanical Engineering
Department, University of
Technology
Baghdad, Iraq
20084@uotechnology.edu.iq

Received on: 18/03/2019
Accepted on: 21/06/2019
Published Online: 25/10/2019

Experimental Investigation of Sub-Cooled Flow Boiling in Metallic Microchannel

Abstract Experiments in microchannel heat sink were carried that examine the deionized water two-phase boiling heat transfer. The heat sink consisted of a single microchannel having 300 μm wide nominal dimensions and 300 μm height (hydraulic diameter of 300 μm). The heat sink formed of oxygen-free copper with 72mm length and 12mm width. Experimental operation conditions spanned the heat flux (78-800) kW/m^2 , mass flux (1700 and 2100) $\text{kg/m}^2\cdot\text{s}$ at 31K subcooled inlet temperature. The boiling heat transfer coefficient is measured, and compared with existing correlations. The results show that higher mass flux leads to a higher boiling heat transfer coefficient and the dominant mechanism is convective boiling. In addition, it was found that an existing correlation provides a satisfactory prediction of the heat transfer coefficient.

Keywords- Metallic Microchannel, Two phase flow, Subcooled flow boiling, heat transfer coefficient.

How to cite this article: S.A. Mohammed and E.M. Fayyadh, "Experimental Investigation of Sub-Cooled Flow Boiling in Metallic Microchannel," *Engineering and Technology Journal*, Vol. 37, Part A, No. 10, pp. 408-415, 2019.

1. Introduction

In recent years, flow boiling through microchannels has attracted lots of interest because, in compact areas, it has a possibility for very elevated heat transfer rates. When wanting lower rates of coolant flow by using the latent heat of the coolant, higher heat fluxes can be dispersed significantly by flow boiling as compared with its single-phase counterpart. The phase variation process happens at the fluid saturation temperature with higher temperature uniformity through the microchannel heat sinks, and that is another characteristic of the convective boiling process. In recent years, two-phase heat transfer properties were studied excessively in particular and fantastic efforts have been made to discover the heat transfer mechanisms on a small scale. However, various heat transfer properties were adduced under various experimental conditions such as working fluid, channel geometry, the used mass flux, and heat flux and saturation pressure, etc. Despite that, there are yet numerous existing problems that limit the additional implementation of the microchannel heat sinks, e.g., the large wall superheats at the onset of nucleate boiling (ONB) [1], the large wall-temperature differences between the channels and along with the channel as well as the instability of the two-phase flow. Subcooled boiling is predominately noticed in a micro-channel heat sink. This method maintain comparatively low wall temperature under highly subcooled conditions and prepare high heat transfer rates. When the hot of the surface is

enough for the formation of bubbles, but the bulk liquid temperature keeps under its saturation value, subcooled flow boiling subsists. The onset of nucleate boiling, ONB is called on the initial consistency of bubbles. Depending on the classical theory [2,3] as the bubbles that created at the wall proceed away from the developing saturation boundary layer, they will condense; on the other hand, the heat transfer between the fluid and the wall will be impacted by the presence of these bubbles. During the high level of subcooling or low heat fluxes, several nucleation sites are active, and a part of the heat is transferred by single-phase convection among patches of bubbles. This system is called partial nucleate boiling. Numerous nucleation sites are activated until fully developed nucleate boiling as the heat flux is increased when the surface turns into totally active for nucleation. Subsequently, the saturated nucleate boiling zone is entered when the saturation boundary layer develops and finally covers the whole channel as the bulk fluid is heated. Subcooled flow boiling is one of the most important parameters that affect the performance of the microchannel heat sink so many investigators study this failed such as Peng and Wang [4] studied deionized water flow boiling in a rectangular evaporator of multi-microchannel made of stainless steel. The channel has an aspect ratio (W/H) equal to 0.86, 60mm length and 0.65 mm hydraulic diameter. The experimental setup was an open-loop, and the liquid subcooling was changed from 40K to 70K. They described that although a fully developed nucleate boiling was noticed from the boiling

<http://dx.doi.org/10.30684/etj.37.10A.5>

2412-0758/University of Technology-Iraq, Baghdad, Iraq

This is an open access article under the CC BY 4.0 license <http://creativecommons.org/licenses/by/4.0>

curve, no bubbles were seen in the channel. They ascribed this phenom to the reality that the channel size was very less as compared with the “minimum evaporating space” wanted for the growth of the bubble. In addition, they did not describe any influence for inlet subcooling and mass flux. Qu and Mudawar [5] published convective boiling mechanisms by an inspected experimental study of 21 micro copper channel with 349 μm hydraulic diameter including (30-60)K inlet subcooling condition at arrange of heat fluxes (400-2400) kW/m^2 and (135-402) kg/m^2 mass fluxes using water as a working fluid. They found the dependence of heat transfer coefficient on mass flux and vapor quality but independent of heat flux. Galvis and Culham [6] studied the water flow boiling characteristics in two various individual copper microchannels that have the same length and aspect ratio but different hydraulic diameter (217 and 419) μm with two various inlet subcooling (50.7K and 54.2 K). The tests were completed with a set of mass fluxes (340 and 1373) kg/m^2 , and (31.7 - 1414) kW/m^2 heat fluxes. They mentioned that the nucleate boiling was the dominant heat transfer mechanisms because of the impact of heat flux upon the heat transfer coefficient while the effect of mass fluxes on the heat transfer coefficient was insignificant. Mehmed [7] tested experimentally flow boiling heat transfer within a rectangular copper individual microchannel with 62 mm length, 1 mm width, and 0.39 mm height. The used working fluid was deionized water, the inlet subcooled and inlet pressure is 11 $^{\circ}\text{C}$ and 115 kpa respectively, with limits of mass fluxes (200 - 800) Kg/m^2 . s, and (56 - 865) kW/m^2 heat fluxes. A high-resolution, high-speed camera was also used to conduct flow visualization. For full mass flux values, the results show that unstable flow boiling happened to begin at the boiling onset. The local heat transfer coefficient relies on heat flux at shallow mass and heat fluxes. During elevated mass flux, the impact of heat flux has not exist with little dependence on vapor quality after the entry region. The impact of mass flux was more complicated. Krishnamurthy and Peles [8] investigated HFE-7000 subcooled flow boiling in a hydraulic diameter of 222 μm , with mass flux and heat fluxes range (350-827) kg/m^2 , (100-1100) kW/m^2 respectively. Channels including an individual line of pin fins; significant heat transfer improvement was obtained and noted that through subcooled boiling the local heat transfer coefficient was larger as compared with the similar single-phase flow. Callizo et al. [9] were studied subcooled flow boiling heat transfer in vertical cylindrical

tubes, including the internal diameter of 0.83, 1.22 and 1.70 mm for refrigerant R-134a experimentally. They examined the impacts of the inlet subcooling, channel diameter, mass flux, heat flux and system pressure on the subcooled boiling heat transfer. They found that the wall superheats at ONB was discovered to be significantly greater as compared with that predicted with correlations for larger tubes. They found that a rise of the mass flux guides for early subcooled boiling and to arise in the heat transfer coefficient. The raises of the mass flux happen in a slight improvement of the heat transfer for fully developed subcooled boiling. Smaller channel diameter, higher system pressure and a higher inlet subcooling, a guide to preferable boiling heat transfer.

The objective of the present work is to discuss the subcooled flow boiling heat transfer of deionized water heated in a single microchannel with 300 μm hydraulic diameter and aspect ratio of 1. This test has been done for various experimental conditions, mass fluxes (1700 and 2100) kg/m^2 . s and heat fluxes range (78-800) kW/m^2 and 31K inlet subcooled temperature.

2. Experimental Apparatus and Data Reduction

1. Experimental Setup

The experimental facility consists of a liquid tank, sub-cooler, peristaltic pump, turbine flow meter, pre-heater, test section, and inline filters. The schematic diagram and a plate of the experimental setup are displayed in Figure 1 and plate 1, sequentially. A chiller unit is used for cooling purposes in the sub-cooler and the condenser. Working fluid was deionized water. Vigorous boiling for about one hour was used for degassing of the deionized water in the liquid tank. In order to release gases that are non-condensable to the atmosphere, the top valve of the condenser was opened. A 7 μm filter was installed to separate all particles in the water before the peristaltic pump in the suit. Then the degassed water was introduced into the test section by pumping and a preheater was used in order to control the working fluid inlet temperature. The microchannel test section is designed and machined from oxygen free copper blocks; hence, the block of the micro-channel test section has dimensions of 12 mm width, 25 mm height and 72 mm length. Single microchannel having a length of 62 mm was cut into the top surface of the copper blocks between the 2 mm diameter inlet and outlet plenum using milling machine at a feed rate of 10 mm/min.

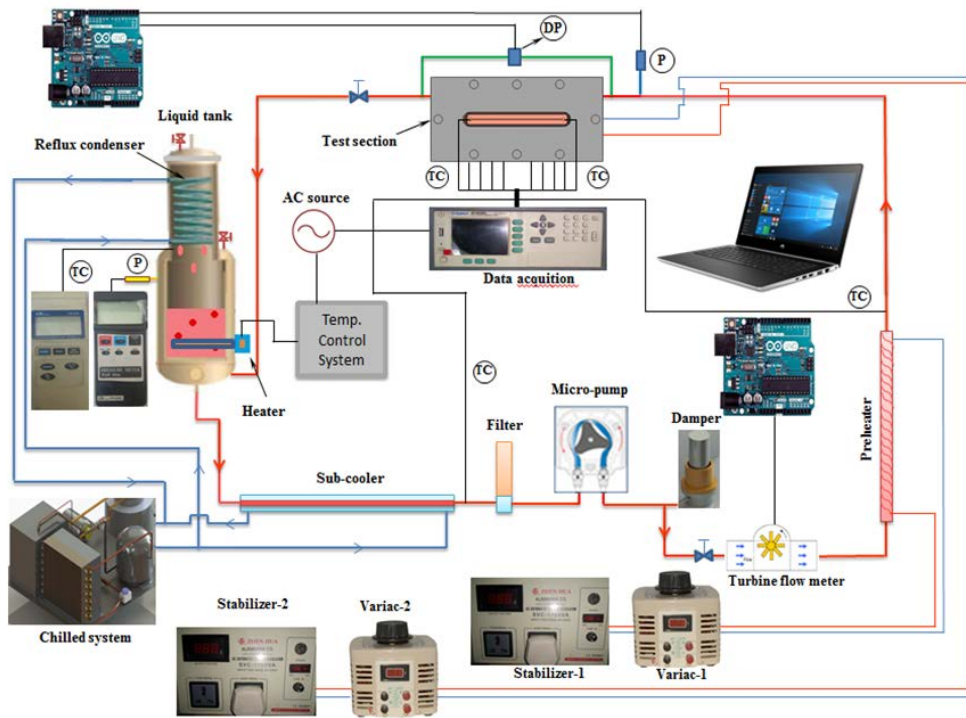


Figure 1: Schematic diagram of the experimental facility.

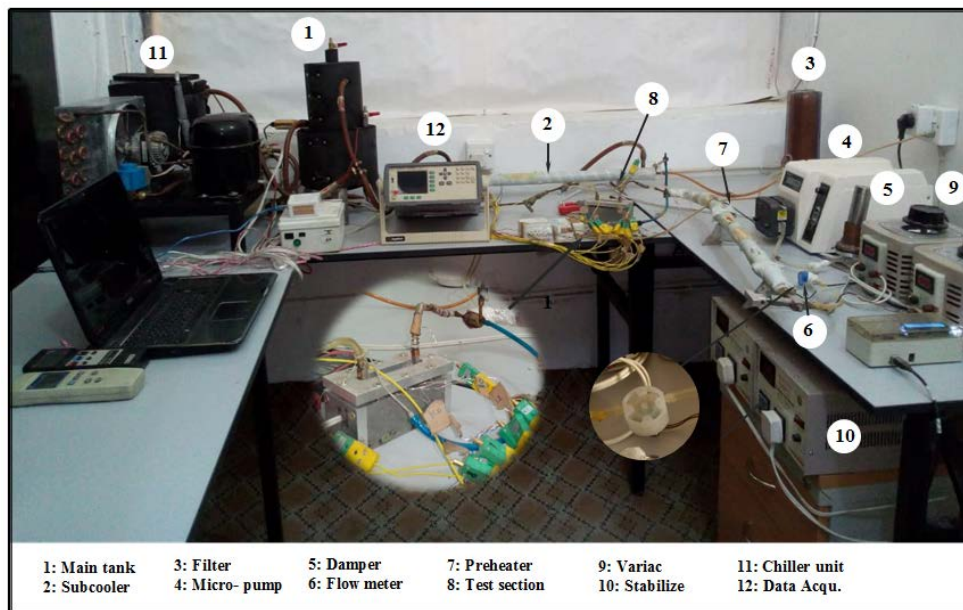


Plate 1: The experimental facility

The typical dimensions of the micro channel are 300- μm width and 300- μm depth. Their dimensions were measured utilizing an electro microscope. The actual dimensions are (367 μm) for width and (269 μm) for height, as shown in Figure 2. The surface roughness at the bottom of the Microchannel test sections was measured with AA3000 Scanning Probe Microscope (Atomic force Microscope AFM contact mode) which has multi-analysis: granularity and roughness. The average surface roughness value is 0.011 μm . Figure 3 shows the roughness values that were evaluated over sample areas of 2cm x 1cm. A

cartridge heater of 250 W heating power was inserted to the copper block at the bottom in a region parallel to the flow, which is placed in a drilled (8mm) hole within the copper block in order to supply the test section with the heating power. The local axial wall temperature was estimated in the 1 mm inner diameter and 6 mm depth hole at the portion of the block of copper.

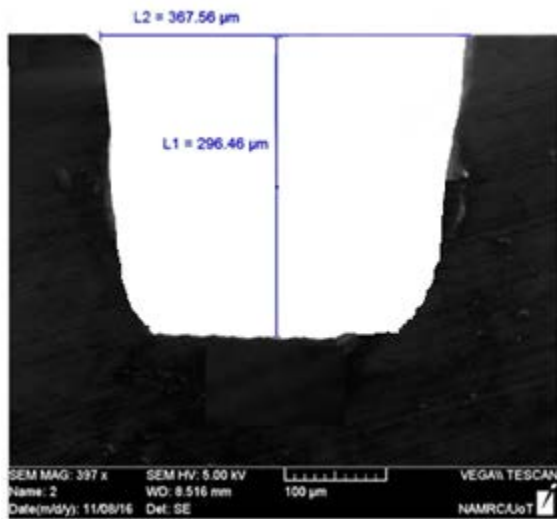


Figure 2: Microscope picture of microchannel

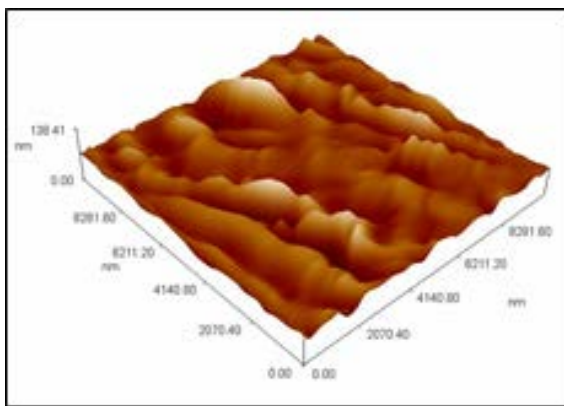


Figure 3: Surface roughness measurements of test section

To estimate the local heat transfer coefficient along the channel, six holes located over the axial side of the channel at equidistance of 12.4 mm with 1 mm from the bottom of the channel to accommodate K-type thermocouples. In addition, from the inlet of the channel with a distance of 24.8 mm, two holes were located vertically and 5 mm below the axial holes with an interval (5) mm. In order to seal leak among microchannels and the top cover, on the top face of the microchannels, an O-ring slot was machined. To reduce heat loss to ambient, the block is inserted into an insulation fiberglass sheet housing; then the assembled is inserted into the housing component, which was designed and manufactured from stainless steel to accommodate the test section in the test loop. Between the stainless steel cover plate and the upper surface of the copper block, 4 mm thickness of the transparent polycarbonate layer was sandwiched. Then two holes were drilled at two locations in the top cover polycarbonate to accommodate thermocouple, one of them at inlet plenum while other at outlet plenum of the microchannel test section.

As well as to accommodate differential pressure drop across the microchannel test sections, Figure 4 presents the main part of the test section.

During the present study, all thermocouples were calibrated with ± 0.5 K of uncertainty. A differential pressure transducer (26pcffT6D) was utilized for estimating the pressure drop, which was calibrated with an uncertainty of ± 0.4 kPa. All information was listed after steady-state condition for 5 min using the Applent AT4532x data acquisition system.

II. Data reduction

1) Single-Phase flow data reduction

ΔP_{ch} , which is the net pressure drop over the microchannel for single-phase flow, is given by:

$$\Delta p_{ch} = \Delta p_{meas} - \Delta p_{loss} \tag{1}$$

ΔP_{meas} represents the total pressure drop among the channel entry and exit plenums. The differential pressure sensor is used to measure it directly. ΔP_{loss} is the pressure loss due to the sudden enlargement and contraction and the inlet and outlet manifolds, and it is described by Eq. (2) below

$$\Delta p_{loss} = 2 \left(\frac{1}{2} \rho_l V_p K_{90} \right) + \frac{1}{2} \rho_l V_{ch} (K_c + K_e) \tag{2}$$

In Eq. (2), V_p represents plenum liquid velocity while V_{ch} represents channel liquid velocity. The direction of entering and leaving flow in the channel is normal to the flow direction. Here, the loss coefficient according to 90° turns of the flow through inlet and outlet plenums, is represented by K_{90} and that is specified by Philips (1987) [10] as 1.2. For the channel entry, and exit, sequentially, K_c is the sudden contraction loss coefficient, and K_e is the sudden enlargement loss coefficient. Tabular data introduced by Shah and London [11] can be used for their values by interpolating.

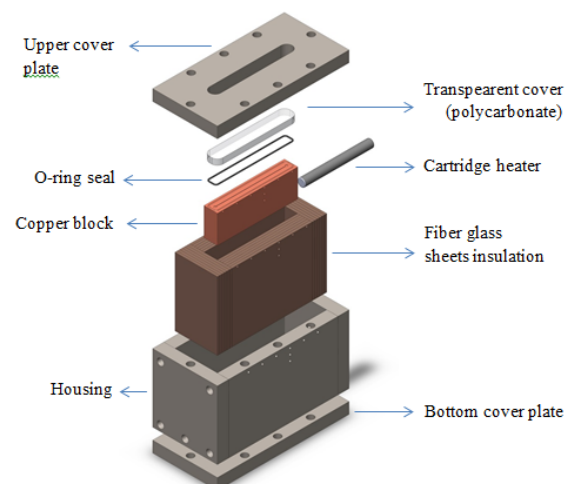


Figure 4: Test section constructions showing the main parts

(hsp(z)) that is the local single-phase heat transfer coefficient as well as (Nu) which is represent the average Nusselt number is determined as:

$$h_{sp}(z) = \frac{q''}{T_w(z) - T_f(z)} \quad (3)$$

$$Nu = \frac{1}{L} \int_0^L \frac{h_{sp}(z) Dh dz}{k_l} \quad (4)$$

Where the channel wall temperature (Tw(z)) at the axial location z was corrected using the 1D heat conduction equation as given by Eq. (5) below. Tf(z) is calculated by Eq. (6) below based on an energy balance assuming uniform heat flux boundary conditions. The heat flux (q'') was defined in Eq. (7).

$$T_w(z) = T_{tc}(z) - \frac{q'' t}{K_{Cu}} \quad (5)$$

$$T_f(z) = T_i + \frac{q'' wz}{m \cdot cp} \quad (6)$$

$$q = \frac{P - Q_{loss}}{A_{ht}} \quad (7)$$

Where: the local thermocouple reading represents by T_{tc}(z), the thermal conductivity of copper represents by k_{Cu}, and the dimension from the channel bottom to the thermocouple position represents by (t) and equal to 1 mm. The temperature of inlet fluid and the specific heat of liquid are represented by T_i and c_p, respectively. The applied electrical power symbolized by P, the heat transfer area represents A_{ht}, and it is calculated by Eq. (8). When there is no fluid inside the test section, an electrical power (P) applies to it in order to evaluate (Q_{loss}) which is the heat loss from the test section. Subsequent achieving steady state, the temperature difference among ambient and the bottom wall was listed for all heating power. After that, in order to achieve an equation to determine the heat loss (Q_{loss}) through single-phase and boiling tests, data obtained from the plotting of the applied power against this temperature difference.

$$A_{ht} = (2H + W) L \quad (8)$$

Where H, W, and L are the high of the channel, the width and the length of it sequentially.

2) Two-Phase flow data reduction

The subcooled liquid state is the condition at which the fluid will coming into the channel. After that, the channel is separated into two regions, single-phase and two-phase. The region that begins from the channel entrance to the position of zero thermodynamic quality represents the single-phase region with length L_{sub}. Therefore, (L_{sat}) which represents the two-phase region length becomes

$$L_{sat} = L - L_{sub} \quad (9)$$

Next equations are used for the calculation of (L_{sub}) which is the length of the single-phase region and it is determined iteratively.

$$L_{sub} = \frac{m cp (T_{sat} - T_i)}{q'' (2H+W)} \quad (10)$$

$$P_{sat(L_{sub})} = p_i - \frac{2f_{app} G^2}{\rho_l D_h} L_{sub} \quad (11)$$

$$f_{app} = \frac{3.44}{Re \sqrt{L''_{sub}}} + \frac{f_{fd} Re + \frac{k}{4 L''_{sub}} - \frac{3.44}{\sqrt{L''_{sub}}}}{Re (1 + C (L''_{sub})^2)} \quad (12)$$

T_{sat} is the liquid saturation temperature while the apparent friction factor that was taken from Shah [12] is represented by f_{app}. Shah [12] introduces the f_{fd}Re, K(∞) and C constant values that are mentioned in Eq. (12) for rectangular channels. (L''_{sub}) that is the dimensionless length in Eq. (12) can be calculated using Eq. (13). (f_{fd}Re) which is represent the fully-developed Poiseuille number is provided by Shah and London [12] in Eq. (14) as a function of channel aspect ratio (β).

$$L''_{sub} = \frac{L_{sub}}{Re D_h} \quad (13)$$

$$f_{fd} Re = 24 (1 - 1.3553\beta + 1.9467 \beta^2 - 1.7012\beta^3 + 0.9564\beta^4 - 0.2537\beta^5) \quad (14)$$

β : is the aspect ratio = 1. In the two-phase section, the local pressure was supposed to reduce linearly with z (the axial length) and it is able to be determined from:

$$P_{sat}(z) = P_{sat}(L_{sub}) - \frac{z - L_{sub}}{L - L_{sub}} \Delta P_{tp} \quad (15)$$

The net pressure drop of the two-phase in the channel is measured from:

$$\Delta P_{tp} = \Delta P_{ch} - \Delta P_{sp} \quad (16)$$

(ΔP_{sp}) which is the pressure drop of the single-phase is able to be calculated depending on Eq. (10) and Eq. (12) that measured the single-phase region length (L_{sub}) and the apparent friction factor respectively. Local heat transfer coefficient of the two-phase was determined as:

$$h_{tp}(z) = \frac{q''}{T_w(z) - T_{sat}(z)} \quad (17)$$

(T_{sat}(z)) temperature in Eq. (17) that is the local saturation is determined depending on the local pressure presented by Eq. (15). (x(z)) is the vapor quality and it was calculated by Eq. (18) and Eq. (19).

$$i(z) = i_l + \frac{q'' (2H+W) z}{m} \quad (18)$$

$$x(z) = \frac{i(z) - i_l(z)}{i_{lg}(z)} \quad (19)$$

Depending on the measured inlet temperature (T_i) and inlet pressure (P_i), the local inlet specific enthalpy i(z) is calculated. In Eq. (19), i_{lg}(z) represents local liquid specific enthalpy while i_{lg}(z) represents local enthalpy of vaporization.

3. Results and Discussions

I. Single-Phase Results

The experiments of single phase were carried previously to experiments of boiling in order to confirm the experimental system. The comparison between the calculated friction factor and the Shah and London [12] correlation for developing and fully developed flow is represented in Figure 5. The figure proves that there is a good contract with correlations. Figure 6 shows the experimental Nusselt number compared with the predictions from the correlations of Shah and London [12]. Mirmanto [13] and mehmed [7]. The experimental values show a similar trend where Reynolds number increases with Nusselt number. However, the current experimental results agree very well with the experimental results of Shah and London [12] for developing laminar flow.

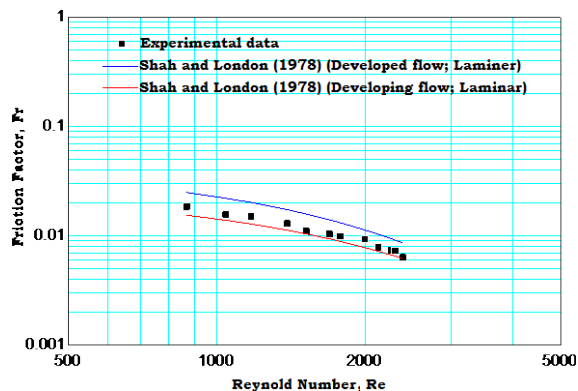


Figure 5: Single-phase results, Fanning friction factor versus Reynolds number

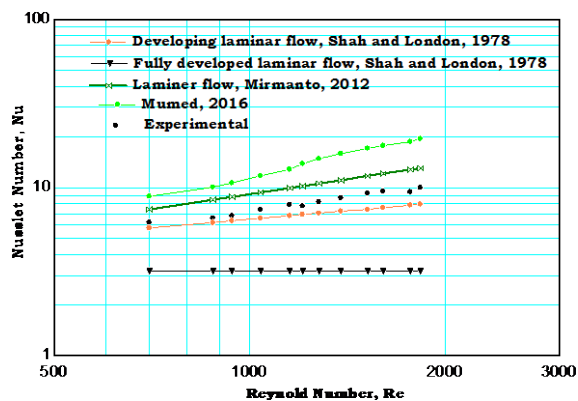


Figure 6: Single-phase results, Nusselt number versus Reynolds number

II. Two-Phase Results

1) Boiling curve

The imposed wall heat flux is plotted against the wall superheat in boiling curves ($\Delta T_{\text{sat}} = T_w - T_{\text{sat}}$) which increases with increasing wall heat flux at constant mass flux. Figure 7 shows the classical boiling curve at the downstream location ($z/l=0.6$) for two different mass fluxes (1700 and 2100) $\text{Kg/m}^2\cdot\text{s}$. The figure divided into two

sections. The first one is the single-phase section where ($\Delta T_{\text{sat}} < 0$), and the second section is a two-phase section where ($\Delta T_{\text{sat}} > 0$). The required heat flux for the commencement of boiling increases with increasing mass flux. Boiling is occurs early when the mass flux is lower.

2) Effect of heat flux on heat transfer

In both micro and macro scale, the impact of heat flux represents an essential part in treating the case of representing predominant flow boiling heat transfer mechanism(s). The nucleate boiling mechanism is assumed to be predominant when a heat transfer coefficient does not vary with vapor quality and mass flux and increases with increasing heat flux. Besides, convective boiling is considered the dominant heat transfer mechanism when the heat transfer coefficient does not depend on heat flux and increases with increasing mass flux and vapor quality. To determine the impact of the heat flux upon the local heat transfer coefficient. Obviously, for the test section, the heat fluxes are divided into two groups the first group with low heat flux values while the others consider as moderate to high heat fluxes. Figures (8 and 9) show the variation of the low heat flux and high heat flux on local two-phase heat transfer coefficient respectively at $1700 \text{ kg/m}^2\cdot\text{s}$ of mass flux, and subcooled inlet fluid temperature is 31 K. In figure 8, the heat transfer coefficient remains in a single-phase region and its increase with increasing heat flux the reason for that the thermal boundary layer was not fully developed. In addition, Figure 8 shows that the heat transfer coefficient increased along the microchannel test part length for the fixed heat flux because of the effect wall temperature of microchannel increase in the axial direction due to the axial heat conduction effect.

Figure 9 depicted a heat transfer coefficient of two-phase as a function of axial distance its shows that for same point increasing heat flux lead to, decreasing the local heat transfer coefficient. The similar outcomes were obtained by a number of researchers such as, Burak Markal et al. [14], Liu et al. [15], as well as Lee and mudawar [1], they reported that the reason for the decrease of two-phase heat transfer coefficient (h_{tp}) with increasing heat flux was due to partially dry out.

3) Effect of mass flux on heat transfer

Figure 10 shows the variation of local heat transfer coefficient with heat flux for two mass fluxes at the position of ($z/l = 0.6$) for the thermocouple.

The figure is divided into two regions subcooled flow boiling region and saturated flow boiling region. The two-phase region starts at the boiling

incipiencies, where the peak value for the heat transfer coefficient is reached then declined sharply. The figure also shows that the heat transfer coefficient increased by increasing mass flux for both the subcooled region and the saturated region at constant heat flux. Moreover the boiling incipience delay for the higher mass flux and need higher heat flux for boiling incipience.

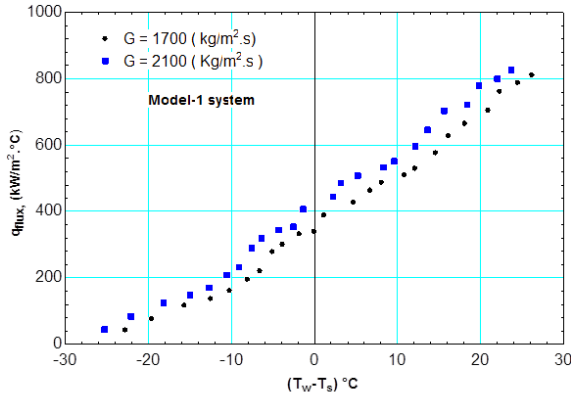


Figure 7: The impact of mass flux upon the boiling curve at 31°C subcooled inlet temperature

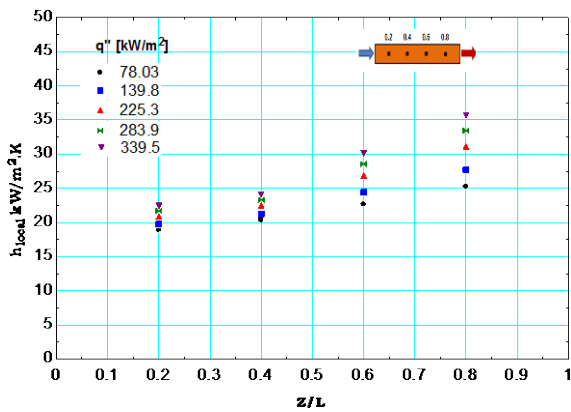


Figure 8: Dimensionless distance from the inlet and low heat flux effectiveness on the local heat transfer coefficient at mass flux of 1700 kg/m².s and subcooled inlet temperature of 31K

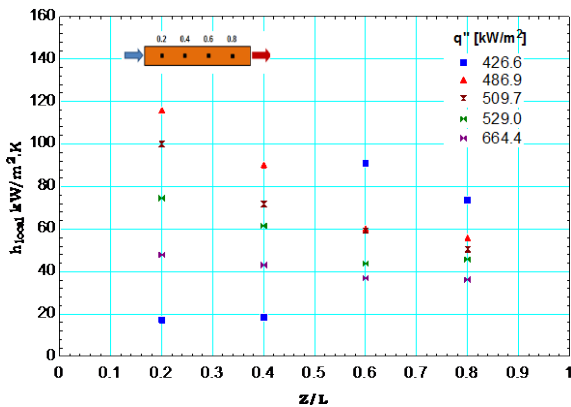


Figure 9: The impact of dimensionless distance from entry and high heat flux upon the Local heat transfer coefficient at a mass flux of 1750 kg/m².s and subcooled entry temperature of 31K

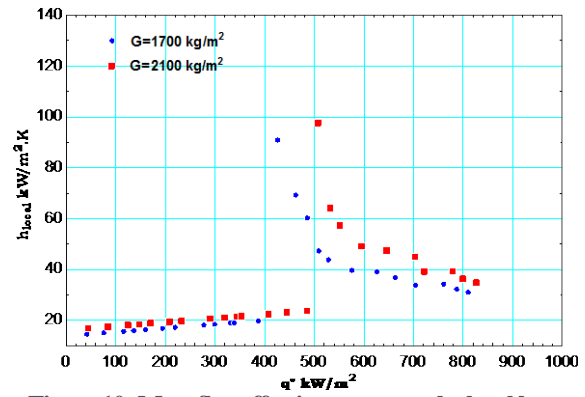


Figure 10: Mass flux effectiveness upon the local heat transfer coefficient at subcooled inlet temperature of 31 K

III. Comparison with Existing Prediction Methods

The heat transfer coefficient divided by two correlations, which is Lee and Mudawar [1] and Mahmoud and Karayiannis [16], is compared with the calculated heat transfer coefficient in the present work. The mean absolute error percentage (MAEP) is used for evaluating the accuracy of each correlation as follows:

$$MAEP = \frac{1}{2} \sum \left| \frac{h_{exp} - h_{pred}}{h_{exp}} \right| * 100 \quad (22)$$

A relationship in a single microchannel having a 0.35 two-phase boiling is suggested by Lee and Mudawar [1]. The points of Data for 318 heat transfer of water and refrigerant R134a are used to depend on it for the correlation. The correlations of Lee and Mudawar [1] give the preferable correlations having minimal than 20 % of mean absolute error, as shown in Figure 11. By utilizing the results of R134a, the relationship of Mahmoud and Karayiannis [16] were advanced of microtubes. They adjusted the convective boiling enhancement factor and the nucleate boiling suppression factor. This correlations predicted lower than the Lee and Mudawar [1] correlation the cause may be attributed to the state of the working fluid that entered the microchannel which is subcooled in Lee and Mudawar [1] which is similar to this study while it is saturated in Mahmoud and Karayiannis [16] as shown in Figure 12.

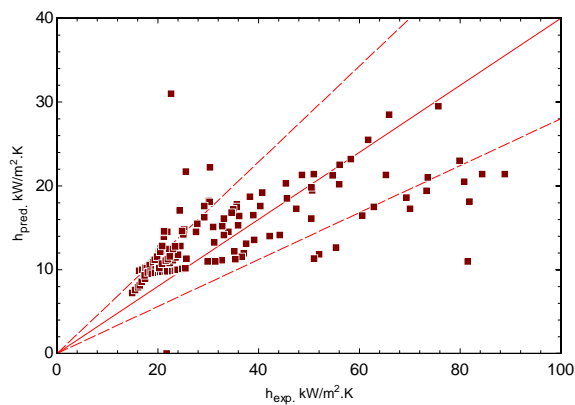


Figure 11: Comparison of experimental heat transfer data with Lee and Mudawar (2005) correlation at mass flux 1700 and 2100 kg/m².s and inlet subcooled 31 °C with MAEP 20%

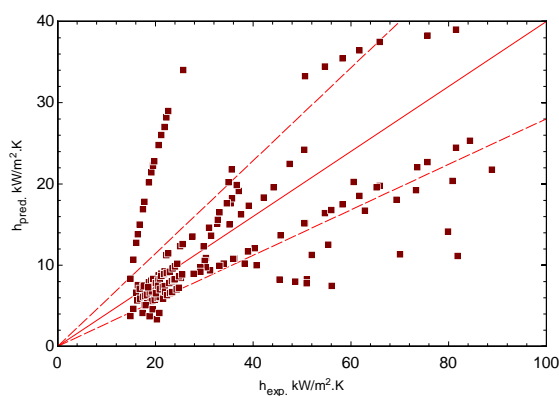


Figure 12: Comparison of experimental heat transfer data with Mahmoud (2013) correlation at mass flux 1700 and 2100 kg/m².s and inlet subcooled 31°C with MAEP% 30

4. Conclusion

The experiments of subcooled flow boiling in a single microchannel heat sink utilizing deionized water were completed at 31 K inlet subcooled for two mass flux (1700 and 2100) kg/m².s and heat flux range (78– 800) kW/m². In this study, the main conclusions drawn from this study are: The correlations of fully developed flow and the conventional scale developing flow in the laminar regime were compatible with the experimental friction factor data. The impact of mass flux was clear on boiling curves, which refer that the mechanism is convective boiling. The results of heat transfer described that heat transfer coefficient based substantially on the heat flux where the two-phase heat transfer coefficient reaches peak value at boiling incipience while in the single-phase region the heat flux has a little effect on heat transfer. In addition, the heat transfer coefficient is increased when the mass flux is increased.

References

[1] J. Lee and I. Mudawar, "Two-phase flow in high heat flux microchannel heat sink for refrigeration cooling applications: Part II-heat transfer characteristics,"

International Journal of Heat and Mass Transfer, 48, 941-955, 2005.

[2] L.S. Tong and Y.S. Tang, "Boiling Heat Transfer and Two-Phase Flow," Second Edition, Taylor & Francis Ltd. London, 1997.

[3] J.G. Collier and J.R. Thome, "Convective boiling and condensation," 3rd Edition (1994) Oxford Science Publications 1-33, 131-182, 183-213, 325-374, 1994.

[4] X.F. Peng and B.X. Wang, "Forced convection and flow boiling heat transfer for liquid flowing through microchannels," International Journal of Heat and Transfer, 36, 3421-3427, 1993.

[5] W. Qu and I. Mudawar, "Flow boiling heat transfer in two-phase micro-channel heat sinks—I," Experimental investigation and assessment of correlation methods, International Journal of Heat and Mass Transfer, 46, 2755-277, 2003.

[6] E. Galvis and R. Culham, "Measurements and flow pattern visualizations of two-phase flow boiling in single channel microevaporators," International Journal of Multiphase Flow, 42, 52-61, 2012.

[7] R. Mehmed, M. Mohamed and G. Tassos, "Flow boiling heat transfer in a rectangular copper microchannel," Journal of Thermal Engineering, 2, 2, 2016.

[8] S. Krishnamurthy and Y. Peles, "Flow boiling heat transfer on micro pin fins entrenched in a microchannel," J. Heat Transfer 132, 4, 04-07, 2010.

[9] C. Martín-Callizo and B. Palm, "Subcooled flow boiling of R 134a in vertical channels of small diameter," International Journal of Multiphase Flow 33, Issue 8, 822-832, 2007.

[10] R.J. Phillips, "Forced convection, Liquid Cooled, Microchannel Heat sinks," MSc thesis, Massachusetts Institute of Technology, Cambridge, USA, 1987.

[11] R.K. Shah and A.R. London, "Laminar flow forced convection in ducts," Oxford Academic Press, New York, USA, Supplement 1 to Advances Heat Transfer, 1978.

[12] R.K. Shah, "A correlation for laminar hydrodynamics entry length solution for circular and non circular ducts," Journal of Fluids Engineering, 100, 177-179, 1978.

[13] M. Mirmanto, "Single-phase flow and flow boiling of water in horizontal rectangular microchannels," Ph.D. thesis, Brunel University London. UK, 2012.

[14] B. Markal, O. Aydin and M. Avci, "Effect of aspect ratio on saturated flow boiling in microchannels," International Journal of Heat and Mass Transfer, 93:130-143, 2016.

[15] D. Y. Liu, X. Weng and X. Guang, "Experimental study on the heat transfer coefficient of water flow boiling in mini/ microchannels," Experimental Thermal and Fluid Science, 35, Issue 7, 1392-1397, 2011.

[16] M.M. Mahmoud & T.G. Karayiannis, "Heat Transfer Correlation For Flow Boiling In Small To Micro Tubes," Int. J. of Heat and Mass Transfer, 66, 553-574, 2013.